# On the Relationship Between Double Bounce and the Orientation of Buildings in VHR SAR Images

Adamo Ferro, *Student Member, IEEE*, Dominik Brunner, *Member, IEEE*, Lorenzo Bruzzone, *Fellow, IEEE*, and Guido Lemoine, *Senior Member, IEEE*

***Abstract*—In this letter, we study empirically the relation between the double-bounce effect of buildings in very high resolution (VHR) synthetic aperture radar (SAR) and the orientation angle for two different ground materials (i.e., asphalt and grass) by analyzing two different TerraSAR-X VHR spaceborne SAR images. Furthermore, we compare our empirical results with the simulations obtained using theoretical electromagnetic models. In order to deal with slightly rough surfaces, we also present a novel model for double-bounce scattering based on the small-perturbation method. We show that the double-bounce effect results in different power signatures, depending on the type of the building and the surrounding ground properties. Finally, we discuss the reliability of theoretical models for predicting the double-bounce power for the analyzed data sets. The models can predict the general behavior of the double bounce but lack in calculating the accurate double-bounce radar cross section reliably.**

***Index Terms*—Double bounce, radar remote sensing, synthetic aperture radar (SAR), urban areas, very high geometrical resolution images.**

## I. Introduction

AMONG THE different scattering contributions present in 1-m-resolution very high resolution (VHR) synthetic aperture radar (SAR) (e.g., COSMO-SkyMed and TerraSAR-X) data from urban areas, the double-bounce effect of buildings (which is caused by the corner reflector assembled by the front wall of the building and its surrounding ground area) is an important scattering characteristic [1], [2]. It indicates the presence of a building because it appears as a linear feature in correspondence with its front wall. The double bounce has been exploited for the development of automatic methods for the detection and reconstruction of buildings from multiaspect [3] and interferometric SAR data [4]. However, the relation between the double-bounce effect and the SAR illumination conditions, and thus its reliability as a feature for building detection purposes, has not been investigated to a sufficient extent in real VHR SAR images yet.

The effect of the orientation angle $\phi$ of a building (i.e., the angle between the front wall of the building and the azimuth direction) on the power signature of the double bounce is important. As an example, we show in Fig. 1 a meter-resolution TerraSAR-X image and the corresponding aerial photograph of a flat-roof building that has two main axes, i.e., it has two walls which are oriented toward the sensor but with different orientation angles. The smaller axis of the building (A) shows a stronger double bounce than the larger axis (B). Since we are investigating the same building, which has similar structures for the two front walls [as shown in Fig. 1(b)], the deviations in the strength of the double bounce cannot be attributed to the differences in either the material properties or the facade structure. Nevertheless, observing the orientation angles with which the two walls were imaged, we find that they are quite different ($\phi = 2.4^\circ$ for A and $\phi = 29.2^\circ$ for B). Another factor that affects the double-bounce scattering is the ground material, whose properties are difficult to retrieve without any *a priori* information about the scene.

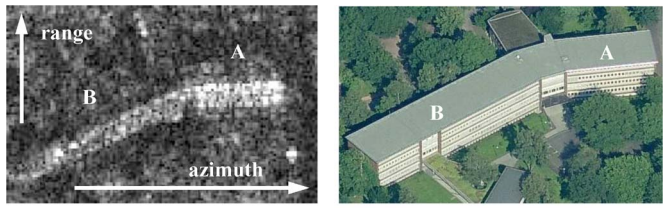


(a) (b)

Fig. 1. (a) Building with two axes in VHR TerraSAR-X data. Illumination from bottom to top (Infoterra, 2008). (b) Corresponding optical image (Microsoft).

As buildings are imaged with different orientation angles in different surroundings, the relation between the orientation angle, the ground material, and the double-bounce strength implies the limits of detection techniques which are based on the double-bounce effect. In this context, the understanding of this behavior both on theoretical models and on real VHR SAR images can be exploited for developing novel optimized detection techniques based on single SAR images [5] and refined tools for the interpretation of the scattering in urban areas [6]. This is of special interest for operational monitoring tasks with stringent limitations on the timely availability of the data (e.g., for emergency response), where the acquisition of a pair of images for building detection cannot be considered.

In this letter, we extend and refine the findings from [7], presenting a detailed study of the relation between the double-bounce effect and the orientation angle. First, we investigate empirically a set of industrial and residential buildings with two different ground materials (grass and asphalt) in ascending and descending spaceborne meter-resolution TerraSAR-X images.

Manuscript received April 30, 2010; revised August 21, 2010 and October 7, 2010; accepted October 29, 2010.

A. Ferro, D. Brunner, and L. Bruzzone are with the Department of Information Engineering and Computer Science, University of Trento, 38123 Trento, Italy (e-mail: adamo.ferro@disi.unitn.it; dominik.brunner@disi.unitn.it; lorenzo.bruzzone@disi.unitn.it).

G. Lemoine is with the European Commission Joint Research Centre, 21027 Ispra, Italy (e-mail: guido.lemoine@ec.europa.eu).

Color versions of one or more of the figures in this paper are available online at http://ieeexplore.ieee.org.

Digital Object Identifier 10.1109/LGRS.2010.2097580

Then, we compare these findings with the state-of-the-art theoretical models in order to assess to which extent they can predict the double-bounce behavior. This is important to consider if these models are employed for information extraction purposes (e.g., building detection and reconstruction). In order to deal with slightly rough surfaces such as asphalt, we developed a novel model for double-bounce scattering based on the small-perturbation method (SPM), which is an improvement of the model previously presented in [7].

## II. Background

### A. Theoretical Models

In order to model the double-bounce effect of a building, the theory of dihedral corner reflectors has been extended to simplified building models, which are generally constituted by rectangular parallelepipeds with smooth walls surrounded by a homogeneous ground surface [1], [2]. These models are considered isolated in the electromagnetic sense, i.e., no interactions with other structures in the scene are taken into account. In particular, Franceschetti *et al.* [1] present a fully analytical electromagnetic model for urban environments that also includes a study on the double-bounce contribution from buildings based on geometric optics (GO) and physical optics (PO) [8], according to the surface roughness.

However, the choice of the adequate roughness parameters, i.e., the rms height $(s)$ and the correlation length $(l_c)$, and dielectric parameters of a surface is nontrivial. Radar cross section (RCS) measurements made directly on SAR images can differ considerably with theoretical predictions using literature material parameters, e.g., due to the effect of the moisture content or the temperature of the material. Furthermore, the surfaces in urban areas are not homogeneous, even at the scale of a single meter-resolution cell. For instance, a paved street in a city may have small-structure elements (e.g., manhole covers), causing local variations in the actual surface roughness. Moreover, they are also made of metal, which is a different material with respect to the surrounding asphalt. Hence, using only the dielectric constant and surface roughness parameters of asphalt to calculate the RCS of a street in urban areas is a significant simplification. In addition, in dense urban environments, scattering effects coming from adjacent objects can interfere and therefore invalidate the assumption of isolated buildings. As a result, the theoretical models currently reported in literature can only be considered as a tool for making preliminary predictions of the scattering behavior of buildings in urban environments, imposing the need for empirical studies.

### B. Empirical Studies

The effect of the orientation angle on the scattering from urban areas (the so-called cardinal effect) has already been reported for medium-resolution SAR data [9]. Furthermore, Hussin [10] demonstrated the influence of polarization and incidence angle on the double-bounce effect, which showed that the corner reflector has, generally, a higher return in HH polarization. Instead, VV polarization is more sensitive to variations in the incidence angle. This analysis was conducted only on buildings that were parallel or perpendicular to the azimuth direction. In [2], the authors discussed the influence of both incidence and orientation angles on the scattering from urban environments using actual SAR airborne data. They observed that the buildings which are parallel to the azimuth direction have a stronger double-bounce contribution than the buildings facing away from the radar. Their study was conducted on a small set of residential and commercial buildings.

Some preliminary experimental studies on the double-bounce effect have been conducted, acquiring SAR measurements on scaled building models under controlled conditions. In [11], the results of an experiment developed by means of an outdoor inverse SAR (ISAR) facility on corner reflector models made from different real-world materials are presented. In [12], we presented a detailed experimental study using polarimetric laboratory ISAR measurements, which were taken on a scaled building model. In addition, we discussed preliminary results for a meter-resolution airborne image which was a simulation of a spaceborne acquisition. Both studies confirmed that the double-bounce effect gives a strong power signature to buildings with walls almost parallel to the SAR azimuth direction but decays rapidly in a narrow range of orientation angles.

## III. Analysis of Real VHR Spaceborne SAR Data

The data that we analyze in this study are a pair of ascending and descending high-resolution spotlight TerraSAR-X images acquired in HH polarization in December 2007 and January 2008 from the city of Dorsten, Germany. Their geometric resolution is 1.1 m $\times$ 1.2 m (azimuth $\times$ slant range). The two images were acquired with similar incidence angles (50.7° for the ascending and 53.8° for the descending image).

This study aims at analyzing the actual double-bounce effect of buildings which are minimally affected by the scattering from other structures present on walls (e.g., metal pipes and porch roofs). For complex building facades, the backscattering depends rather on the elements on the facades than on the double-bounce effect itself. In fact, such elements may interfere with the double wall–ground and ground–wall reflections. Therefore, we selected a set of candidate buildings which presented simple walls (i.e., no windows and balconies) with asphalt or grass ground surfaces in the surroundings using the bird's eye view data from Bing maps. We estimated their planar and height dimensions from the optical images in order to predict their scattering behavior. These estimates were then confirmed by measuring the return of the buildings on the SAR image. The expected scattering behavior of a building permitted to locate the position of the double-bounce stripe, the layover and shadow areas, and the eventual single-bounce stripe due to an inclined building roof.

The data set included 55 buildings suitable for the extraction of the mean RCS value of the expected double-bounce area: 17 residential buildings surrounded by asphalt terrain (*residential/asphalt*), 19 industrial buildings surrounded by asphalt terrain (*industrial/asphalt*), and 19 residential buildings surrounded by grass-covered soil (*residential/grass*). We considered buildings with different orientation angles in the range between 0° and 42°. For larger orientation angles, the double-bounce areas of suitable buildings were not well distinguishable from the surroundings; thus, we did not consider these buildings in the study. In single polarized images,

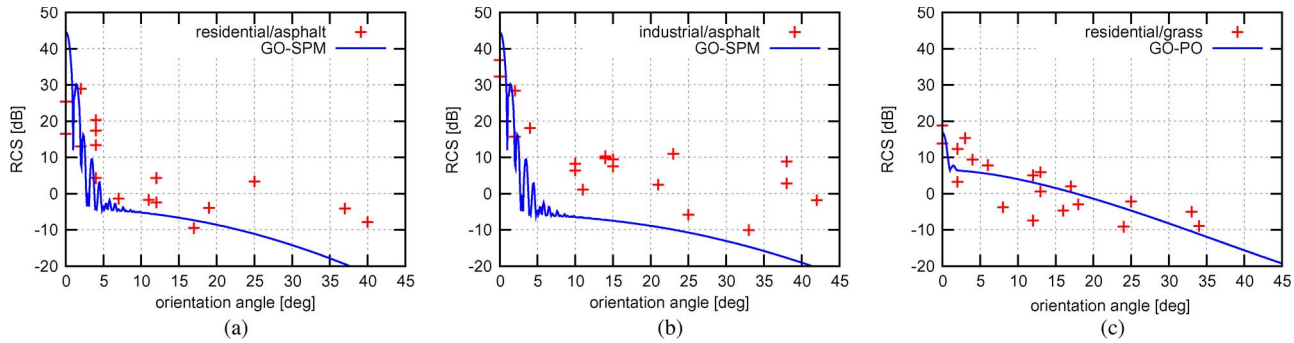


Fig. 2. Relation between double-bounce RCS and orientation angle: (Crosses) Collected data and (solid line) theoretical model. (a) *Residential/asphalt* category. (b) *Industrial/asphalt* category. (c) *Residential/grass* category.

single-bounce backscattering from the building roofs complicates the extraction of the double-bounce stripes, as in many cases, this contribution is superimposed with the double-bounce stripe itself. In our observations, this occurs mainly when the roof is not facing the SAR sensor and appears to be related to the roof tile coverage. Buildings showing a single-bounce stripe overlapping with the expected double-bounce region have not been considered in our analysis. The RCS of the double bounce is dependent on the area of the building wall and, thus, also on its height. The higher the building, the stronger the double bounce. This needs to be taken into account when the RCSs of different buildings are compared to each other. As the empirical measurements refer to buildings with different heights, we considered as reference a building height of 6.5 m, which is the mean height of the buildings in the data set, and normalized the RCS values accordingly. The normalization has been performed taking into account the quadratic and linear dependences of the double-bounce RCS on the building height for coherent and incoherent scatterings, respectively [1], [2]. As the azimuth resolution is smaller than the building length, we did not consider the length in the normalization step [1]. The difference of the incidence angles between the two scenes is about 3°. Based on theoretical models, we confirmed that this variation in incidence angle only implies a marginal change of the double-bounce RCS, which can be assumed to be smaller than the error introduced by the analysis process. Hence, we considered the buildings in the two scenes as they were in a single scene.

The results of the analysis are shown in Fig. 2 (crossed points), which shows the relation between the RCS of the corner reflector and the orientation angle per building/terrain category. The graphs show that buildings with similar orientation angles can have double-bounce stripes that differ by several decibels. This behavior reflects the fact that, in real SAR data, many variables (which are mainly unknown) affect the scattering behavior of surfaces, as mentioned in Section II. Therefore, our goal was to analyze the overall trend of the double-bounce effect for each class of buildings, rather than the double-bounce stripe of individual buildings.

Fig. 2(a) shows the behavior of the RCS versus the orientation angle for the *residential/asphalt* case. The graph shows that, on the one hand, the double bounce is significant in the first 10° orientation angle range, with values on the order of 30 dB, and then decreases considerably. The strong part of the double bounce is caused by a strong coherent scattering. On the other hand, for larger orientation angles, the relevance of incoherent scattering due to the surface roughness increases, and the double-bounce effect is less pronounced. The results of the analysis of the *industrial/asphalt* class are shown in Fig. 2(b). The trend is similar to that for the *residential/asphalt* class but with generally higher power values. The difference is on the order of 10 dB. Moreover, the double bounces of the buildings in the *industrial/asphalt* class present a sparser distribution. These two effects can be explained by the variable and inhomogeneous materials used for industrial buildings and by the presence of more metal parts that are not as common as those for residential buildings. Finally, Fig. 2(c) shows the distribution of the double-bounce RCS for the *residential/grass* class. Due to the impact of the roughness of the grass surrounding the buildings (which is expected to be higher than that for asphalt grounds), the contrast between the double-bounce peak at near-0° orientation angles and the remaining part of the graph is lower than that for buildings which are surrounded by asphalt. The peak power is about 10 dB lower compared to that for the *residential/asphalt* class, while the RCS decreases with increasing orientation angles in a smoother way, suggesting a pronounced relevance of incoherent scattering.

## IV. Comparison Between Empirical Results and Theoretical Models

### A. Theoretical Models

In order to assess whether the trends shown in Section III are in agreement with theoretical models, we compared the actual data to simulated data obtained with analytic models. The models approximate the building wall as a smooth surface in order to apply standard GO rules for the estimation of the scattering from the wall. This allows the calculation of the area which is illuminated at the ground in closed form by considering a plane wave reflected by the wall. Hence, no roughness parameters need to be defined for the wall. The area surrounding the building wall is considered as a rough surface. On the one hand, the roughness parameters of grass allow for the considered frequency the estimation of the double-bounce scattering power for the *residential/grass* class using the GO–PO approximation proposed in [1]. On the other hand, the analytic models currently reported in the literature are not valid for slightly rough surfaces like asphalt. Therefore, we derived a novel model for double-bounce scattering based on GO–SPM. The single backscattering contribution of the ground and its eventual variations are not taken into account, as they

are expected to be negligible compared with the double-bounce power for the considered incidence angle [1].

For the double-bounce modeling, both formulations are composed of two contributions: a coherent ($\sigma_{\mathrm{DB},c}$) and an incoherent term ($\sigma_{\mathrm{DB},i}$). The double-bounce RCS is obtained by the sum of these two contributions. For the proposed GO–SPM model, the coherent term corresponds to the scattering from a smooth dihedral corner reflector on an infinite surface

$$\sigma_{\mathrm{DB},c} = \left(\frac{k^2}{\pi}\right) A_W^2 |S_{hh}|^2 \mathrm{sinc}^2\left[kl\sin(\theta)\sin(\phi)\right] \cdot \mathrm{sinc}^2\left[kh\frac{\sin^2(\theta)\sin^2(\phi)}{\cos(\theta)}\right] \quad (1)$$

where $k = 2\pi/\lambda$; $\mathrm{sinc}(x) = \sin(x)/x$; $h$ and $l$ are the height and length of the wall, respectively; and $A_W = hl\tan(\theta)\cos(\phi)$. The term $S_{hh}$ is defined by

$$S_{hh} = 2R_{\perp}(\theta)\cos(\theta)\cos(2\phi)A_h + \left[\sin^2(\theta)\sin(2\phi) + R_{\parallel}(\theta)\left(1+\cos^2(\theta)\right)\sin(2\phi)\right] B_h \quad (2)$$

$$A_h = -\cos^2(\theta)\cos^2(\phi)R_{\perp W}(\theta_W) + \sin^2(\phi)R_{\parallel W}(\theta_W) \quad (3)$$

$$B_h = \cos(\theta)\cos(\phi)\sin(\phi)\left[R_{\perp W}(\theta_W) + R_{\parallel W}(\theta_W)\right] \quad (4)$$

where $R_{\perp}(\theta)$, $R_{\parallel}(\theta)$ and $R_{\perp W}(\theta_W)$, $R_{\parallel W}(\theta_W)$ depict the Fresnel coefficients for the ground and the wall, respectively. $\theta_W = \cos^{-1}[\sin(\theta)\cos(\phi)]$ is the local incidence angle on the building wall. The incoherent scattering is given by

$$\sigma_{\mathrm{DB},i} = 32A_W|\alpha_{hh} + \alpha_{hv}|^2\cos^4(\theta)k^4s^2 \cdot W\left\{k\sin(\theta)\left[1-\cos(2\phi)\right], -k\sin(\theta)\sin(2\phi), l_c\right\} \quad (5)$$

where $W(k_x, k_y, l_c)$ represents the roughness spectrum using a Gaussian correlation function and is given by

$$W(k_x, k_y, l_c) = \frac{l_c^2}{2}\exp\left[-\frac{l_c^2}{4}\left(k_x^2 + k_y^2\right)\right]. \quad (6)$$

The factors $\alpha_{hh}$ and $\alpha_{hv}$ are given by

$$\alpha_{hh} = -A_h\frac{(\varepsilon_{\mathrm{ground}} - 1)\cos(2\phi)}{(\cos(\theta) + C)^2} \quad (7)$$

$$\alpha_{hv} = B_h\frac{(\varepsilon_{\mathrm{ground}} - 1)\sin(2\phi)C}{(\cos(\theta) + C)(\varepsilon_{\mathrm{ground}}\cos(\theta) + C)} \quad (8)$$

where $C = \sqrt{\varepsilon_{\mathrm{ground}} - \sin^2(\theta)}$ and $\varepsilon_{\mathrm{ground}}$ is the dielectric constant of the ground surface.

Both the GO–PO and GO–SPM models do not consider the effects of the azimuth aperture of the SAR sensor in order to achieve a simple analytical solution [13]. These contributions are expected to be negligible for the scope of this letter [1].

### B. Dielectric and Roughness Parameters

To compare the results from the empirical analysis with theoretical models, we first collected the information about the roughness parameters and the dielectric characteristics of the materials (asphalt, grass, and concrete) from the literature (see Table I) [14], [15]. Starting from these values, we calculated the theoretical curves which give the minimum rmse with respect to the data from the real SAR images for each of the three categories. The fitting has been performed in the validity ranges of the considered theoretical models [8]. The calculated best fit parameters are reported in Table II.

TABLE I
ROUGHNESS PARAMETER AND DIELECTRIC CONSTANT RANGES USED FOR THE FITTING OF THE THEORETICAL MODELS TO THE MEASURED DATA ($\varepsilon = \varepsilon' - j\varepsilon''$)

| **Materials** | $\varepsilon'$ | $\varepsilon''$ | $s$ | $l_c$ |
|---|---|---|---|---|
| Asphalt | 3–8 | 0–0.5 | 0.3–1.4 mm | 0.4–2 cm |
| Grass | 3–20 | 0–7 | 5–20 mm | 0.5–10 cm |
| Concrete | 3–8 | 0–0.5 | - | - |

TABLE II
MATERIAL PROPERTIES AND MAE BETWEEN EMPIRICAL AND THEORETICAL RCSS PER CATEGORY

| | *residential/asphalt* | *industrial/asphalt* | *residential/grass* |
|---|---|---|---|
| **Building wall** | $\varepsilon = 8.0 - j0.5$ | $\varepsilon = 8.0 - j0.5$ | $\varepsilon = 4.0 - j0.05$ |
| **Ground surface** | $\varepsilon = 8.0 - j0.5$<br>$s = 1.4$ mm<br>$l_c = 1.8$ cm | $\varepsilon = 8.0 - j0.5$<br>$s = 1.4$ mm<br>$l_c = 1.5$ cm | $\varepsilon = 14.0 - j1.0$<br>$s = 10$ mm<br>$l_c = 5.5$ cm |
| **MAE** | | | |
| **0° - 10°** | 16.40 dB | 14.06 dB | 4.73 dB |
| **11° - 45°** | 8.40 dB | 15.17 dB | 3.91 dB |
| **0° - 45°** | 12.18 dB | 14.79 dB | 4.25 dB |

### C. Analysis of Results

The solid lines in the graphs in Fig. 2 show the theoretical RCSs as a function of the orientation angle in comparison to the measured data from the actual SAR scenes. In Table II, the mean absolute error (MAE) between empirical and theoretical RCSs (in decibels) is reported. Considering the graph for the *residential/asphalt* category [Fig. 2(a)], the range in which the coherent term prevails matches correctly with the points characterized by high RCS values for small orientation angles. However, for large orientation angles, the theoretical model underestimates the double-bounce power. Considering the orientation angles between 11° and 45°, the empirical mean power is −2.74 dB, and the MAE is 8.40 dB. The prediction error of the theoretical model is thus considerable. Note that the best fit curve is obtained using the upper limits of the parameter ranges for the dielectric constants and for $s$ (see Table II). Using higher values for these parameters results in a better fit. However, this would imply that the materials are not realistic. Moreover, higher $s$ values do not fulfill the SPM validity conditions [8]. The *industrial/asphalt* category [Fig. 2(b)] shows characteristics that are similar to those of the *residential/asphalt* case. The prediction error for large orientation angles is higher than that for small orientation angles. In fact, the MAE for orientation angles greater than 10° is equal to 15.17 dB, while the empirical mean power in the same range is 3.80 dB. Considering the *residential/grass* category [Fig. 2(c)], the theoretical curve has a good agreement with the empirical data. The contribution of the coherent scattering term is reduced

to the first orientation angles, and its strength is much lower than those for the *residential/asphalt* and *industrial/asphalt* classes, as expected, due to the increased surface roughness of grass with respect to asphalt.

For asphalt surfaces, the use of the literature values in the theoretical models did not reflect the behavior of the empirical measurements sufficiently, particularly for high orientation angles. This can be explained by the presence of metal objects or other small structures, resulting in a relatively strong scattering also at larger orientation angles. For the grass surfaces, the GO–PO model can predict the scattering behavior of the selected buildings more accurately. However, the range of valid model parameters for grass is very large (see Table I), hampering a precise *a priori* choice of reasonable general values. This confirms that, as mentioned in Section II, the scattering in urban areas depends on many variables. Literature values for one material are too specific to describe an extended surface in an urban area precisely. Therefore, material properties can only be used in an approximate way in the currently reported analytical electromagnetic models to infer the rough scattering behavior in an urban area in practical situations.

## V. Conclusion

In this letter, we have presented an empirical study on the behavior of the double-bounce scattering mechanism of buildings in VHR SAR. We focused on the analysis of the strength of the double bounce with respect to the orientation angle. The study investigated three classes of buildings in two TerraSAR-X images and compared these results with theoretical electromagnetic scattering models. In this context, we presented a novel model for predicting the double-bounce power based on SPM, which is suitable for urban surfaces like asphalt.

The results pointed out that the double-bounce effect has a strong power signature for buildings which have the wall on the sensor close side almost parallel to the SAR azimuth direction. Furthermore, the strength of the double bounce decays rapidly in a narrow range of orientation angles, while it decays moderately for larger angles. The exact characteristic of the decay depends on the material and surface parameters, making the double bounce a variable feature within the same scene. Therefore, the double-bounce feature can only be used for reliable building detection and reconstruction by taking into account its nonlinear relation with the orientation angle.

The comparison between the predictions from the theoretical electromagnetic models based on SPM and PO and the real data showed that the general behavior of the double bounce can be derived with the theoretical models. However, the complexity of the actual scene hampers the reliable calculation of the double-bounce RCS. In particular, in complex environments such as urban areas, many scattering contributions from small structures with possibly different materials interfere, which is not considered in the currently reported theoretical models. In order to improve their reliability, more complex models need to be developed, including these additional contributions. Nonetheless, although the development of these models is very important from a theoretical viewpoint, the increased number of parameters required by more complex models would make it impossible to use them in real building detection/reconstruction applications.

The study presented in this letter demonstrated that the correct behavior of the double-bounce effect with respect to the orientation angle of buildings can be derived empirically considering a few real-world cases. This result can be integrated easily in practical feature extraction application scenarios, e.g., for the development of building detection/reconstruction techniques from meter-resolution SAR images.

## Acknowledgment

The authors would like to thank F. Greßler from Infoterra, Germany, for providing the TerraSAR-X data. At the time of this research, D. Brunner was with the Department of Information Engineering and Computer Science, University of Trento and also with the European Commission Joint Research Centre.

## References

[1] G. Franceschetti, A. Iodice, and D. Riccio, "A canonical problem in electromagnetic backscattering from buildings," *IEEE Trans. Geosci. Remote Sens.*, vol. 40, no. 8, pp. 1787–1801, Aug. 2002.

[2] Y. Dong, B. Forster, and C. Ticehurst, "Radar backscatter analysis for urban environments," *Int. J. Remote Sens.*, vol. 18, no. 6, pp. 1351–1364, Apr. 1997.

[3] F. Xu and Y.-Q. Jin, "Automatic reconstruction of building objects from multiaspect meter-resolution SAR images," *IEEE Trans. Geosci. Remote Sens.*, vol. 45, no. 7, pp. 2336–2353, Jul. 2007.

[4] A. Thiele, E. Cadario, K. Schulz, U. Thoennessen, and U. Soergel, "Building recognition from multi-aspect high-resolution InSAR data in urban areas," *IEEE Trans. Geosci. Remote Sens.*, vol. 45, no. 11, pp. 3583–3593, Nov. 2007.

[5] A. Ferro, D. Brunner, and L. Bruzzone, "Building detection and radar footprint reconstruction from single VHR SAR images," in *Proc. IEEE IGARSS*, Honolulu, HI, Jul. 25–30, 2010, pp. 292–295.

[6] R. Guida, A. Iodice, D. Riccio, and U. Stilla, "Model-based interpretation of high-resolution SAR images of buildings," *IEEE J. Sel. Topics Appl. Earth Obs. Remote Sens.*, vol. 1, no. 2, pp. 107–119, Jun. 2008.

[7] D. Brunner, L. Bruzzone, A. Ferro, and G. Lemoine, "Analysis of the reliability of the double bounce scattering mechanism for detecting buildings in VHR SAR images," in *Proc. IEEE RadarCon*, Pasadena, CA, May 4–8, 2009, pp. 1–6.

[8] F. T. Ulaby, R. K. Moore, and A. K. Fung, *Microwave Remote Sensing: Active and Passive*, vol. 2, *Radar Remote Sensing and Surface Scattering and Emission Theory*. Norwood, MA: Artech House, 1982.

[9] G. Hardaway and G. C. Gustafson, "Cardinal effect on SEASAT images of urban areas," *Photogramm. Eng. Remote Sens.*, vol. 48, no. 3, pp. 399–404, 1982.

[10] Y. A. Hussin, "Effect of polarization and incidence angle on radar return from urban features using L-band aircraft radar data," in *Proc. IEEE IGARSS*, Florence, Italy, Jul. 10–14, 1995, pp. 178–180.

[11] T. Kempf, M. Peichl, S. Dill, and H. Süß, "Microwave radar signature acquisition of urban structures," in *Proc. ITG WFMN*, Chemnitz, Germany, Jul. 4–5, 2007, pp. 68–73.

[12] D. Brunner, L. Bruzzone, A. Ferro, J. Fortuny, and G. Lemoine, "Analysis of the double bounce scattering mechanism of buildings in VHR SAR data," in *Proc. SPIE Conf. Image Signal Process. Remote Sens. XIV*, Cardiff, U.K., Sep. 15–18, 2008, vol. 7109, pp. 710 90Q–710 90Q–12.

[13] A. S. Khwaja, L. Ferro-Famil, and E. Pottier, "Efficient SAR raw data generation for anisotropic urban scenes based on inverse processing," *IEEE Geosci. Remote Sens. Lett.*, vol. 6, no. 4, pp. 757–761, Oct. 2009.

[14] E. J. Jaselskis, J. Grigas, and A. Brilingas, "Dielectric properties of asphalt pavement," *J. Mater. Civil Eng.*, vol. 15, no. 5, pp. 427–434, Sep./Oct. 2003.

[15] T. Jackson, H. McNairn, M. Weltz, B. Brisco, and R. Brown, "First order surface roughness correction of active microwave observations for estimating soil moisture," *IEEE Trans. Geosci. Remote Sens.*, vol. 35, no. 4, pp. 1065–1069, Jul. 1997.